2007 IEEE International Conference on
Robotics and Automation
Roma, Italy, 10-14 April 2007

Autonomous Robotic Sensing Experiments at San Joaquin River

Amarjeet Singh*, Maxim A. Batalin*, Victor Chen*, Michael Stealey*, Brett Jordan†, Jason C Fisher‡, Thomas C. Harmon‡, Mark H Hansen§ and William J Kaiser*

*Department of Electrical Engineering, University of California, Los Angeles.
‡School of Engineering, University of California, Merced
†Department of Mechanical Engineering, University of California, Los Angeles
§Department of Statistics, University of California, Los Angeles

Abstract— **Distributed, high-density spatiotemporal observations are proposed for answering many river related questions, including those pertaining to hydraulics and multi-dimensional river modeling, geomorphology, sediment transport and riparian habitat restoration. In spite of the recent advancements in technology, currently available systems have many constraints that preclude long term, remote, autonomous, high resolution monitoring in the real environment. We present here a case study of an autonomous, high resolution robotic spatial mapping of cross-sectional velocity and salt concentration in a river basin. The scientific objective of this investigation was to characterize the transport and mixing phenomena at the confluence of two distinctly different river streams - *San Joaquin River* and its tributary *Merced River*. Several experiments for analyzing the spatial and temporal trends at multiple cross-sections of the *San Joaquin River* were performed during the campaign from August 21-25, 2006. These include deterministic dense raster scans and in-field adapted experimental design. Preliminary analysis from these experiments illustrating the range of investigations is presented with the focus on adaptive experiments that enable sparse sampling to provide larger spatial coverage without discounting the dynamics in the phenomena. Lessons learned during the campaign are discussed to provide useful insights for similar robotic investigations in aquatic environments.**

I. INTRODUCTION

River observations are important from the perspectives of navigation, water supply, flood control, water quality monitoring and management. Water managers in many of the arid or semi arid regions, such as Western U.S., rely on quantitative water distribution algorithms to balance the needs of municipalities, farms, flood control and aquatic ecosystems. Deterministic river flow and transport models can play a role in determining optimal distributions. However, lack of advances in sensing systems often resulted in usage of overly simplified routing models for regulatory work. These routing models are often calibrated using time series data from a network of river gauging stations which record gross flow and, in some cases, temperature and bulk salinity in terms of the water's electrical conductivity (EC) [1].

One such example is San Joaquin river basin in Central California where a robust network of 14 river gauging stations with a spatial granularity of tens of kilometers is operated and maintained by government agencies. Several factors such as water resources, population influxes, land use changes and climate change impacts [2] create a demand for high density, distributed observation of flow and water quality parameters. Such observations will enable distributed model parameterization and enable more detailed water quality forecasting than had been possible in the past. This will also provide policy-makers with the information to make more informed decisions about issues extending beyond water supply and flood control to the restoration of river habitat and aesthetics.

Several prototype sensing systems have been used for sensing the aquatic systems at different scales. Buoyed or moored deployment platforms exist which can provide vertical profiling capabilities over long time periods at key locations [3], [4]. Networked Aquatic Microbial Observing System (NAMOS) [5] employs a system of static buoys equipped with chlorophyll sensor along with an array of 6 thermistors, each at different depths and a boat equipped with fluorometer and thermistor to provide water surface measurements. The system in its current form has limited capabilities in terms of providing cross-sectional phenomena distribution.

Autonomous underwater vehicles (AUVs) have been used extensively by the oceanographic community, and more recently in lakes and large rivers [6]. However, greater currents and confined operating space associated with small to moderately sized rivers limit the applicability of AUVs in these systems. The Rivernet monitoring program is an effort towards providing high resolution (temporal) measurement of nitrate using in-stream nutrient analyzers [7]. However the instrumentation measures a single point within the flow stream and hence only provides temporally high resolution data, without any spatial resolution. In spite of the recent advancements in technology, currently available systems have many constraints that preclude long-term, remote, autonomous, high-resolution monitoring in the real environment. These include availability of energy, precise autonomous actuation, precise localization, data communication and others. Researchers commonly survey stream velocity by manual operations, for example suspending sensors from bridges [8] or performing high resolution flow field characterization of river cross-section using laser doppler anemometer [9]. Literature survey reveals that this is for the first time that such an extensive set of experiments have been performed using an autonomous robotic system, performing high resolution spatial mapping of cross-sectional velocity and salt concentration in a river basin.

Such high granularity and autonomous measurements were made possible using a cable based robotic system - Networked Info Mechanical System (NIMS), introduced in [10]. A Rapidly Deployable (RD) version, NIMS-RD (Fig. 1), was developed to fill the void for efficient and high granularity

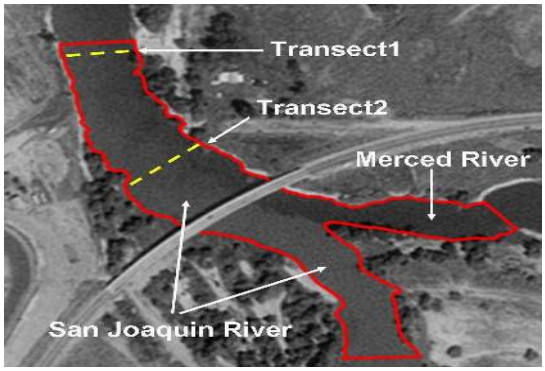

(a) Campaign site

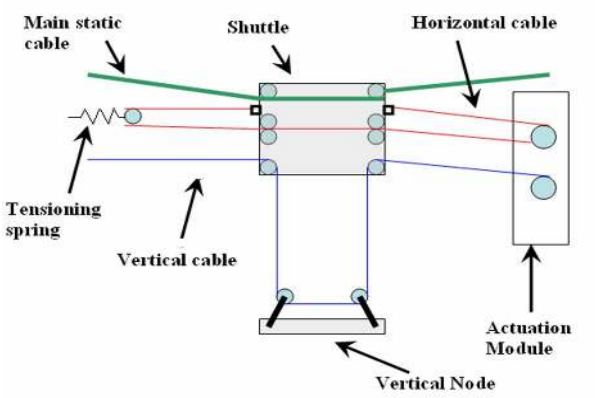

(b) Schematic view with basic cable setup

Fig. 1: Satellite view of campaign site and schematic diagram of NIMS system used for autonomous sampling

two dimensional mapping. In this paper we provide a case study of a campaign at San Joaquin river for mapping the river cross-sectional velocity and salinity, executed from August 21-25, 2006 with NIMS-RD. Fig. 1a displays the satellite view of the campaign site. We performed autonomous robotic sensing experiments at the multiple cross-sections and collected physical samples for detailed lab analysis. Real time data collection facilitated high temporal resolution data. Autonomous motion of the mobile system facilitated high spatial resolution data. The high resolution data was then used for preliminary analysis to learn the spatial distribution. This was followed by several adaptive experiments based on learned phenomena distribution. Detailed analysis of such adaptive experiments is presented in this paper to motivate the requirement of sparse sampling, coupled with efficient robotic systems, to provide larger spatial coverage without discounting the dynamics in the phenomenon distribution.

II. NIMS-RD: Infrastructure Supported Autonomous Robotic System

An actuated sensor system, NIMS-RD [11] (hereafter called NIMS), was used during the campaign to navigate a sensor payload anywhere within the two dimensional cross-section of the river. Fig. 1b displays the schematic diagram of the system. It is comprised of three main cables, the mounting hardware, actuation module and a shuttle. The three cables are: the static cable supporting the shuttle and the vertical node platform, a horizontal and a vertical cable used to control the corresponding motion of the sensor payload. The mounting hardware is supported by the static cable and is used to attach the actuation module at one transect end and horizontal and vertical cables at the other end. The shuttle and the vertical node platform are actuated using two motors located on one side of the transect, through the horizontal and the vertical cables. Both of these motors are controlled simultaneously using a serial interface.

This system architecture is an improvement from first generation system introduced in [10]. It allows for reduced node mass, increased horizontal and vertical node speed, constant and convenient access to the actuation control module and rapid yet flexible deployments. Use of cable based system enabled precise localization and ability to actuate heavy sensor payload. System design rationale and implementation

Fig. 2: Complete set of sensors with physical sampling device

details are provided in [11]. Sensing at the lowest point close to the river floor without damaging the sensor system was made possible through accurate depth profiling.

Deflection in the static cable due to system weight may disturb the localization calibration of the system. Winches were used to increase the tension on the static cable to avoid excessive cable deflection, thereby facilitating long term autonomous motion resulting from accurate localization. The cable is specified to support a maximum tension of 3700 pounds while the maximum tension on our system was close to 750 pounds which was well within the safety limits. Tensioning spring at one end keeps the horizontal cable loop tight and prevents it from slipping on the spool on the other side. The vertical cable was tensioned manually. This proved to be sufficient, since the vertical cable was also kept under tension by the sensor payload.

Vertical festooning connected to the sensor system comprised of the data and the power cables. Power was delivered to the sensor system using a multi conductor cable. Serial interfaces from the sensor system were supported using a serial to ethernet bridge interface, supported by an embedded control and sampling system. Power supply, power control, sensor interface and long range communication were all integrated into a sensor node supported, along with the sensor payload, and by the NIMS system. Real time data monitoring was performed at the near shore side to ensure that data from each sensor is collected autonomously without any error. Several factors including real time data streaming

Sensor type	Sensing Parameter	Sensing Rate	Power Requirements
Hydrolab Minisonde 4a [12]	Temperature, pH, specific conductivity	0.1 Hz (internal logging), 1 Hz (logging over serial port)	External AC power and/or battery (AA) power
Hydrolab DS5 [12]	Depth, oxidation reduction potential, turbidity, Luminescent Dissolved Oxygen (LDO)	0.1 Hz (internal logging), 1 Hz (logging over serial port) Simultaneously logs internally and over serial port	External AC power and/or battery (C) power
ISUS sensor [13]	Nitrate	1 Hz (over serial port) No memory for internal logging	External AC power
Argonaut-ADV [14]	Flow velocity	0.1 Hz (both internal and serial port logging) Simultaneously logs internally and over serial port	External AC power

TABLE I: Description of sensors used during the campaign

and monitoring, sufficient AC power for the payload devices, accurate depth profiling and precise localization among others enabled autonomous motion of the robotic system.

Several sensors used at different stages of the campaign for monitoring different phenomena are described in Table I. Detailed characterization of the sensed phenomena may be constrained by the available sensors. In spite of recent advances in commercially available sensors for aquatic monitoring, certain characteristics still require detailed lab analysis using physical samples of water collected from the river. To facilitate such analysis, a physical sampling device was developed to collect water samples in the field from any desired location. The device uses dual spring loaded syringes to collect water samples when actuated at any location within the two dimensional cross-section of the river. In consultation with the environmental scientists, we learned that a sample quantity of approximately 30 ml is sufficient for detailed laboratory analysis of most phenomena of interest in this application area. Our device collects approximately 70 to 80mL of water, in two syringes, at a time ensuring that at least twice the required amount of water samples are collected from each desired location to account for errors during lab analysis. It uses a system that triggers the action of a spring-loaded device controlled by a solenoid actuated by the sensor node power system. Fig. 2 shows the picture of all four sensors and the physical sampling device.

III. Experimental Design

The scientific objective of this investigation was to characterize the transport and mixing phenomena at the confluence of two distinctly different rivers: the Merced River (relatively low salinity) and the agricultural drainage-impacted San Joaquin River (relatively high salinity). High spatial resolution sensing experiments were performed at two different transects. Fig. 1a displays the two transects in the satellite image of the campaign site. The first transect was selected further downstream from the confluence point of San Joaquin river and Merced river (approximately 290 meters downstream) and was representative of the conditions within the downstream portion of the confluence mixing zone. The second transect was selected upstream closer to the confluence of the two rivers (approximately 130 meters from the confluence point). This was representative of the conditions in the upstream portion of the confluence mixing zone. Approximate widths of the two transect was 50 meters and 70 meters respectively.

Deterministic dense scans with uniform sampling density

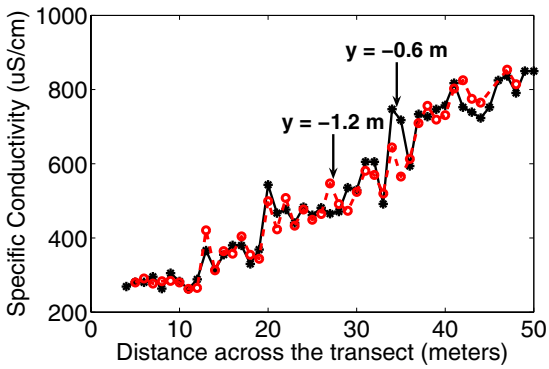

Fig. 4: Spatial variation of specific conductivity at two different depths during the raster scan in the morning of August 23.

(i.e raster scans) were performed at both transects. Sampling density for the scan was selected to be 1 meter across the river and 0.6 meters along the depth. This density was decided in consultation with environmental scientists based on prior experiences in sensing such phenomena distribution [15]. This resulted in a total of 250 and 293 observation locations in the two transects respectively. Dwelling time at each sensing location was fixed to 30 seconds to comply with the requirements associated with both the settling time of sensor systems and the requirement to collect multiple samples at each location to verify sampling stability. Fixing the dwelling time also ensured uniformity across several raster scans at both transects. However, with such an experimental configuration, it took approximately 158 and 185 minutes to complete a single raster scan at the two transects respectively. Accurate modeling of such environments require making these observations over large spatial domain as well as incorporating the spatiotemporal dynamics of the phenomena distribution. This motivated the need for adaptively sampling the environment. This involves performing sparse sampling to provide larger spatial coverage without discounting the spatiotemporal dynamics in the phenomena. We performed several in-field adapted experiments, described next, and detailed analysis from such experiments is presented as a study of the trade off between sensing time and sensing accuracy.

The first adaptive approach that we studied was a common approach from spatial statistics based on a rich class of probabilistic models called Gaussian Processes (GPs) [16]. Using GP based approach, we quantified the informativeness of a particular location, in terms of the uncertainty about our prediction of the phenomena at the unobserved locations, given the observations from already visited locations. To

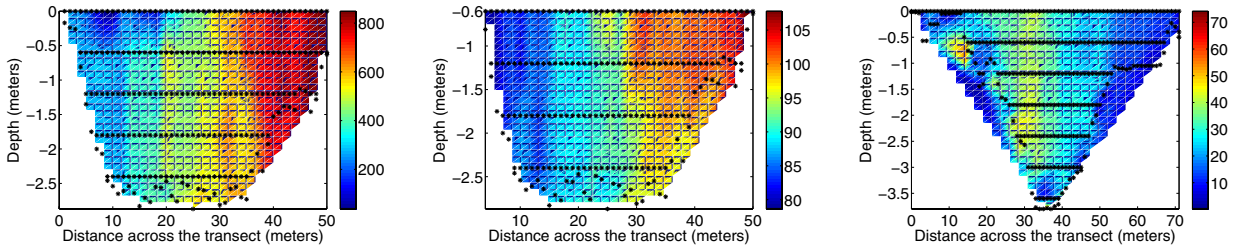

(a) Specific conductivity at the first transect during raster scan on August 23 morning (b) Nitrate at the first transect during raster scan on August 23 evening (c) Flow distribution at the second transect during raster scan on August 25 morning

Fig. 3: High granularity (raster) scans at the two transects for different parameters

quantify this uncertainty, we use the mutual information (MI) criterion [17]. If the phenomenon is discretized into finitely many sensing locations $\mathcal{V}$, then for a set of locations $\mathcal{P}$ visited by the mobile robot, the MI criterion is defined as:

$$\mathrm{MI}(\mathcal{P}) \equiv H(\mathcal{X}_{\mathcal{V}\setminus\mathcal{P}}) - H(\mathcal{X}_{\mathcal{V}\setminus\mathcal{P}} \mid \mathcal{X}_{\mathcal{P}}), \qquad (1)$$

where $H(\mathcal{X}_{\mathcal{V}\setminus\mathcal{P}})$ is the entropy of the unobserved locations, and $H(\mathcal{X}_{\mathcal{V}\setminus\mathcal{P}} \mid \mathcal{X}_{\mathcal{P}})$ is the conditional entropy after observing sensing locations $\mathcal{P}$. Therefore, mutual information measures the reduction in uncertainty at the unobserved locations. In particular, we learned a non-stationary GP model by maximizing the marginal likelihood [16] using the specific conductivity data for half (125 locations out of the total of 250) of the observation locations from the raster scan. We then used the mutual information criterion to greedily select a set of 30 and 50 locations each, from the remaining 125 locations. Based on the observations from this subset of locations, specific conductivity at the remaining locations was predicted using the learned model.

As a measure of trade off between sensing time and prediction accuracy, we also reduced the density of observation locations and predicted the phenomena at the rest of the locations using simple interpolation. It was observed that specific structure in the phenomena distribution (vertical stratification) could be exploited to reduce the density of observation locations with very little reduction in prediction accuracy.

Logging the data in real time using the serial port connectors on the sensors provided several advantages. This increased the logging rate for both Hydrolab Minisonde-4a and Hydrolab DS5. Additionally, logging in real time ensured robustness against the system failure which could simply be detected based on graphical visualization. We monitored the data in real time and it helped us at several occasions when we were able to detect certain faults in real time and were able to take immediate remedial actions.

IV. Results and Discussion

We present here the analysis from several experiments performed during the campaign. Several spatial and temporal trends in the distribution of observed phenomena are presented to display the spatiotemporal dynamics.These observed dynamics motivated the experimental design involving several adaptive approaches discussed in Section III. Detailed analysis from these experiments is presented in Section IV-C to further motivate the requirement for efficient experimental design in addition to the robust and autonomous robotic sensing system. Piecewise bilinear interpolation is performed between the sampling locations to create the surface distributions. For each surface distribution, the mean at each location is considered as the sampled value at that location. Points in the surface distributions, wherever applicable, represent the observation locations. As per the coordinate system, x-axis represent distance along the cross-section of the river, while y-axis represent distance along the depth ($y = 0$ represent the water surface). The water stream on the near side (lower x coordinate value) is coming from Merced river while the water stream on the far side is coming from San Joaquin river.

A. Spatial Trends

Spatial distributions of three of the several measured parameters observed during high granularity raster scans are shown in Fig. 3. Fig. 3a displays the distribution of specific conductivity ($\mu S/cm$) as measured using Minisonde-4a at the first transect during a raster scan performed on the morning of August 23. For precise visualization of the variation along the cross-section, the corresponding spatial distribution at two different depths of 0.6 meters and 1.2 meters is presented in Fig. 4. Fig. 3b shows the distribution of nitrate concentration ($\mu Mol/L$) as measured by the ISUS sensor along the same cross-section during the evening of August 23. Due to the difference in the lengths of ISUS and Minisonde-4a, ISUS sensor was above the river surface for all the observations taken at $y = 0$. Therefore, only the readings for depths less than 0 are considered for creating the surface distribution.

Strong vertical correlation can be easily observed from all surface distributions as well as from the comparison of specific conductivity curves at different depths. Additionally, from the surface distributions it can be clearly observed that there exists a vertical stratification with three different zones. Two zones on either end represent individual streams from San Joaquin river and Merced river while the middle one represent the confluence mixing zone.

Fig. 3c shows the flow distribution (cm/s) as measured by Argonaut-ADV along the cross-section of the second transect on the morning of August 25. As expected, there is near zero flow close to each bank and close to the river floor, while there is a uniform flow in the middle of the river.

B. Temporal Trends

Fig. 5 shows temporal variation of specific conductivity as observed during several experiments. Fig. 5a shows the distribution of specific conductivity at a depth of 1.2 meters across raster scans performed on August 23 and August 24

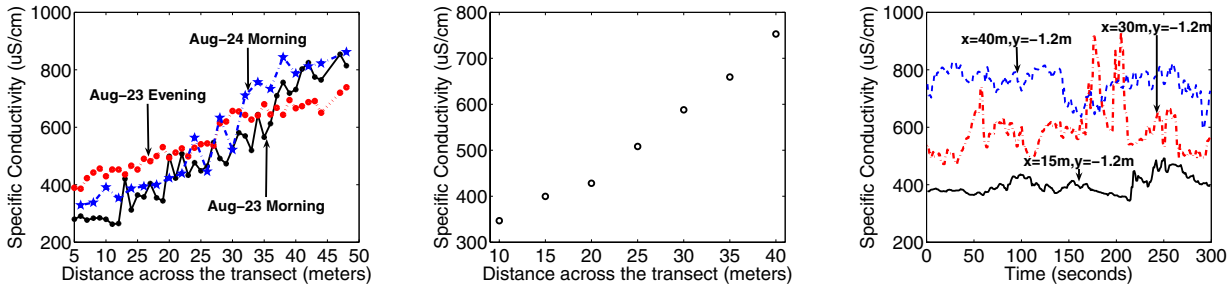

(a) Variations at 1.2 meters depth during different raster scans

(b) Short term mean across the transect

(c) Short term variations at three locations

Fig. 5: Temporal trends for specific conductivity at the first transect

at the first transect. This displays the long term temporal trends over consecutive days for the distribution of specific conductivity. As can be observed, there is considerable difference not just across different times during the day but also across same time for consecutive days.

To analyze the short term temporal trends of the phenomena distribution, we selected a set of 7 locations at a depth 1.2 meters below the water surface. At each location we increased the dwell time to 5 minutes. Fig. 5b shows the mean value during the dwelling time of 5 minutes at different locations along the cross-section of river. Fig. 5c shows the corresponding time series measured at a distance of 15, 30 and 40 meters during the duration of 5 minutes. As is clear from the plots, there is considerable temporal variation even in a short duration of 5 minutes, especially towards the far side of the river. It can be observed that the time series for each spatial point has different characteristics (much more extreme excursions in the middle than at the edges). This further motivates adaptive dwelling time based on dynamics in the phenomena distribution.

C. Adaptive Sampling

Fig. 6 shows the distribution of specific conductivity when a sparse sampling density is considered at the first transect. Fig. 6a displays the distribution of specific conductivity when sparse density is considered along the cross-section, keeping the density along the depth same. Fig. 6b represents the distribution of specific conductivity when sparse density is considered along the depth keeping the density along the cross-section same. Each of these two scans present an interpolation from a subset of locations from dense raster scan, performed on morning of August 23 are considered. These surface distributions visually appear similar to those created using the complete set of observation locations. This is a preliminary indication that the phenomena shows a smooth distribution with no abrupt peaks. Thus, a model based approach can be effectively used to perform sparse sampling without neglecting the spatiotemporal dynamics.

Since the phenomena displayed vertical stratification, an intuitive adaptive approach would be to reduce the observation density along the y axis by a larger magnitude compared to reduction in observation density along the x axis. This simple experiment was executed on August 24 around the same time as the dense scan demonstrated in Fig. 3a. It resulted in observations at a total of 85 locations. Additionally, we observed that dwelling time at each observation location can be reduced to 15 seconds without significant reduction in prediction accuracy. With this reduced dwelling time total experiment time, including the observation and travel time, for this scan was approximately 36 minutes. Fig. 6c displays the surface distribution produced using data observations from this scan. The difference in the interpolated surface, when compared to the surface distributions created from experiments on August 23, can be attributed to the temporal variations in the phenomena distribution. These temporal variations are discussed in detail in Section IV-B.

As a preliminary testing of a model based adaptive approach, we trained a GP using a subset of locations from the raster scan performed on August 23. Next NIMS-RD performed observations at the greedily selected subset of locations. Consequently the phenomena is reconstructed by predicting the values at the unobserved locations using the learned model and observed values. Finally the complete set of values, predicted and sampled, are interpolated to generate the surface distribution. Fig. 7a and Fig. 7b display the predicted surface when 30 and 50 locations are selected respectively out of a total of 250 locations. These locations are selected greedily based on Mutual Information criterion discussed in Section III. Total time duration for observing at 30 locations was approximately 20 minutes while for 50 locations it was approximately 31 minutes. This is considerably smaller when compared with 158 minutes for the complete raster scan. Thus, learning a model for phenomena distribution and accordingly performing an adaptive sensing could save a lot of experimental time.

To estimate the accuracy of prediction using the GP based approach, we need ground truth about the phenomena distribution as the reference. To estimate this ground truth data, we neglected the temporal variation across consecutive days and used the data from the raster scan experiment at approximately the same time the previous day. Fig. 7c represents the distribution of specific conductivity as was sampled during the raster scan, at approximately the same time during the previous day. The predicted surface using the GP based approach appears visually similar to the actual phenomenon distribution. Still, there is considerable difference between the predicted surface and the ground truth. This could be attributed to several reasons. The primary reason based on our analysis is the temporal variation in the phenomena distribution. The model was learned based on a

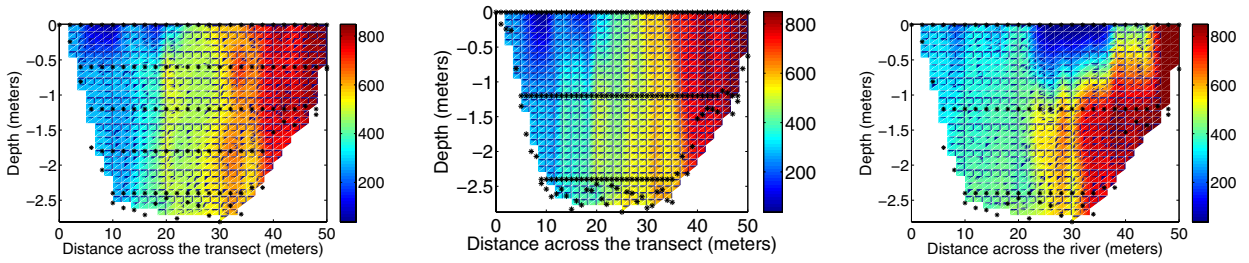

(a) Sparse sampling across the transect (b) Sparse sampling along the depth (c) sparse sampling using the NIMS system

Fig. 6: Effect of sparse sampling on specific conductivity at the first transect

raster scan performed at the previous day during a different time of the day. The model in its current form, does not take into account the temporal variations in the phenomena distribution. This may lead to inaccuracy in estimating the subset of observation locations in predicting the phenomena at unobserved locations. Another reason for the non smooth surface distribution can be the bilinear interpolation used for creating these surfaces. These are only the preliminary results from one of the several adaptive experimental design approaches we intend to study during our future deployments for modeling the distribution of several phenomena.

D. Physical Sampling

The physical sampling device was used to collect water samples from several locations along the cross-section of the first transect. Several lab tests show detectable amounts of boron and phosphate, elements interesting to the environmental scientists but can not be detected using the currently available suite of sensors. Additionally, we also tested the collected samples for nitrate concentration and the measurements were well in accordance with the measurements taken by ISUS sensor in the river. This further validated the calibration of the sensor and precision of the autonomous collection of physical water samples.

V. Lessons Learned

The application of autonomous robotic sensing in complex river system environments presents a wide range of challenges that are not encountered in laboratory systems. While the described experimental campaign, employing the NIMS robotic system, has provided data of immediate value to the urgent environmental investigations, it has also provided lessons that will advance next versions of the actuated sensing systems (such as NIMS). Specific structure in the observed phenomena motivated the requirements for adaptive experiment design and efficient robotic system to effectively sense larger spatial domains without discounting the spatiotemporal dynamics.

Campaign experience had shown that selection of specific deployment sites should be done very carefully accounting for all the system constraints. For a cable based robotic system requiring support infrastructure, availability of suitable anchoring system should be the primary concern for the choice of deployment site. This requires detailed inspection of each of the sites prior to the deployment to ensure availability of necessary infrastructure. It also permits advance installation of the anchoring system, adapting to the unforeseen circumstances. For our campaign, the deployment sites were inundated by flood waters merely a few months prior to this deployment rendering the soil incapable to support heavy system infrastructure. Each of the two deployment sites were chosen based on the availability of natural (trees) or man made (steel towers) infrastructure used in addition to our anchoring system to support the heavy cable based system.

Cable based robotic system in the real environment may interfere with the routine work of the individuals using the same environment. In our case, some of the fishermen used to go around in the boats in the river later in the day. Setting up the system each morning and taking it down in the evening is a cumbersome process that should be avoided. This is another criterion that should be kept in mind while selecting the possible sites for the deployment. At out first transect (where we performed most of our experiments) we supported our cable infrastructure with another cable, at more suitable height, running between the the two steel towers that were already in place.

The use of cable based robotic system introduces high precision in transport. However, to exploit this capability over long transects (spanning over 50 meters), deployment design limits must be incorporated. First, the essential horizontal and the vertical drive cables enabling the corresponding motion of the sensing node, require an appropriate tension. A low tension on either of these cables would cause non-deterministic cable motion due to a slipping action encountered at the cable actuators. High tension at the cable results in extra load on the motor system. This results in excessive motor actuator heating and ultimately a need to disable these devices during operation for protection. To avoid this problem, the NIMS design incorporates tensioning spring at one end of the horizontal cable. This provides sufficient tension on the cable, while at the same time ensures that the tension does not overheat the motors.

Nature brings with it the severe conditions that cause degradation to equipment resulting in in-field failure, not typically encountered in laboratory environment. This is critical to avoid, since the value of acquired data is high and critical to the end users. First, electronic components and infrastructure components must be protected from moisture and be also equipped to withstand indefinite immersion in potentially corrosive water solutions. Further sources of failure are associated with the integrity of data transmission

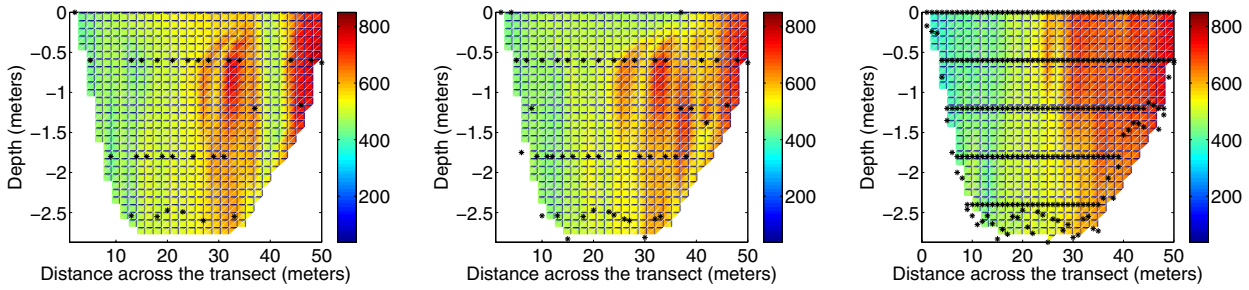

(a) Greedy selection of 30 locations (b) Greedy selection of 50 locations (c) Raster scan

Fig. 7: Predicted distribution of specific conductivity at the cross-section of the first transect using Gaussian Process based modeling and comparison with the distribution sampled by raster scan around the same time, the previous day

cables and connectors. An essential step is the introduction of redundancy in the data capture. This was accomplished by applying both real time monitoring (relying on data transmission cables) as well as the simultaneous archiving of data in the sensor systems themselves using the nonvolatile memory storage. Finally, reliability of sensor node power systems presents yet another concern. Thus, in addition to local energy storage in primary batteries, power is also supplied to sensors to provide a long-term, reliable power source. All of these design features proved to be essential for the success of the campaign described here.

VI. Conclusions and Future Work

In this paper we described a case study for an autonomous, high resolution robotic aquatic sensing and its deployment in an important river system. Experimental investigations were directed to resolve important phenomena in river environment. Several experiments varying from deterministic, dense uniform scans for estimating spatial trends to experiments for estimating the temporal trends were performed during the campaign at San Joaquin river. Specific structure in the observed phenomena (vertical stratification) motivated the requirement for adaptive experimental design in addition to efficient robotic system to effectively sense larger spatial domains without discounting the spatiotemporal dynamics. From an environmental science perspective, this campaign produced coupled velocity and water quality assessments at previously unobservable spatial resolution. Coupled distributions enable precise estimation of chemical fluxes and mass balances, which assist environmental scientist to better understand and model contaminant mixing, reaeration, and other hydraulics-based processes [9], [18] Physical water samples were collected using the autonomous robotic system, from several locations and depths in the river providing a measure of contaminant concentration for those components not detectable by the available sensor suite.

Important lessons learned during the campaign provided a rich set of insights into the preparation for any future campaign in aquatic monitoring. These are currently used for guiding further advances in autonomous NIMS, and can be applied to any cable based robotic sensing systems. Additionally, preliminary analysis from adaptive experimental design further motivated the development and verification of other adaptive approaches, optimized for river system monitoring, that is currently underway. To make the system completely autonomous, efforts are also directed to make several associated operations such as calibration and depth profiling also autonomous.

Acknowledgment

This material is based upon work supported in part by the US National Science Foundation (NSF) under Grants ANI-00331481. Any opinions, findings, and conclusions or recommendations expressed in this material are those of the authors and do not necessarily reflect the views of the NSF. The authors also acknowledge the support of Henry Pai, Yeung Lam, Jon Binney, Andre Encarnacao and Ignacio Zendejas for the system development and deployment during the campaign.

References

[1] "Calsim ii simulation of historical swp-cvp operations," *California Department of Water Resources Technical Memorandum Report*, '2003.
[2] L. D. Brekke, N. L. Miller, K. E. Bashford, N. W. Quinn, and J. A. Dracup, "Climate change impacts uncertainty for water resources in the san joaquin river basin, california," *Journal of the American water resource association*, vol. 40, pp. 149–164, February 2004.
[3] J. V. Reynolds-Fleming, J. G. Fleming, and J. Richard A. Luettich, "Portable autonomous vertical profiler for estuarine applications," *Estuaries*, vol. 25, pp. 142–147, 2004.
[4] K. W. Doherty, D. E. Frye, S. P. Liberatore, and J. M. Toole, "A moored profiling instrument," *Journal of Atmospheric and Oceanic Technology*, vol. 16, pp. 1816–1829, 1998.
[5] A. Dhariwal, B. Zhang, B. Stauffer, C. Oberg, G. S. Sukhatme, D. A. Caron, and A. A. Requicha, "Networked aquatic microbial observing system," in *IEEE ICRA*, 2006.
[6] D. R. Blidberg, "The development of autonomous underwater vehicles (auvs); a brief summary,," in *IEEE ICRA*, 2001.
[7] B. P. Usry, "Nitrogen loading in the neuse river basin, north carolina: The rivernet monitoring program," Master's thesis, North Carolina State University, 2006.
[8] B. De Serres, A. Roy, P. Biron, and J. Best, "Three-dimensional structure of flow at a confluence of river channels with discordant beds," *Geomorphology*, vol. 26, pp. 316–335, 1999.
[9] J. Boxall and I. Guymer, "Analysis and prediction of transverse mixing coefficients in natural channels," *Journal of Hydraulic Engineering*, vol. 129, no. 2.
[10] R. Pon, M. Batalin, J. Gordon, M. Rahimi, W. Kaiser, G. Sukhatme, M. Srivastava, and D. Estrin, "Networked infomechanical systems: A mobile wireless sensor network platform," in *IPSN'05*, pp. 376–381.
[11] B. L. Jordan, M. A. Batalin, and W. J. Kaiser, "Nims rd: A rapidly deployable cable based robot," in *IEEE, ICRA*, 2007.
[12] [Online]. Available: http://www.hachenvironmental.com
[13] [Online]. Available: http://www.satlantic.com
[14] [Online]. Available: http://www.sontek.com
[15] T. C. Harmon, R. F. Ambrose, R. M. Gilbert, J. C. Fisher, M. Stealey, and W. J. Kaiser, "High resolution river hydraulic and water quality characterization using rapidly deployable networked infomechanical systems (nims rd)," *Environmental Engineering Science*, 2006.
[16] M. Seeger, "Gaussian processes for machine learning," *Int. Jour. of Neural Systems*, vol. 14, no. 2, pp. 69–106, 2004.
[17] C. Guestrin, A. Krause, and A. P. Singh, "Near-optimal sensor placements in gaussian processes," in *ICML*, 2005, pp. 265–272.
[18] D. Ho, P. Schlosser, and T. Caplow, "Determination of longitudinal dispersion coefficient and net advection in the tidal hudson river with a large-scale, high resolution sf6 tracer release experiment," *Environmental Science and Technology*, vol. 36, no. 15.